Real-Time Quality Assessment of Videos from Body-Worn Cameras

Yuan-Yi Chang
Centre for Intelligent Sensing
Queen Mary University of London
London, UK
y.chang@se16.qmul.ac.uk

Riccardo Mazzon
Centre for Intelligent Sensing
Queen Mary University of London
London, UK
r.mazzon@qmul.ac.uk

Andrea Cavallaro
Centre for Intelligent Sensing
Queen Mary University of London
London, UK
a.cavallaro@qmul.ac.uk

***Abstract*—Videos captured with body-worn cameras may be affected by distortions such as motion blur, overexposure and reduced contrast. Automated video quality assessment is therefore important prior to auto-tagging, event or object recognition, or automated editing. In this paper, we present M-BRISQUE, a spatial quality evaluator that combines, in real-time, the Michelson contrast with features from the Blind/Referenceless Image Spatial QUality Evaluator. To link the resulting quality score to human judgement, we train a Support Vector Regressor with Radial Basis Function kernel on the Computational and Subjective Image Quality database. We show an example of application of M-BRISQUE in automatic editing of multi-camera content using relative view quality, and validate its predictive performance with a subjective evaluation and two public datasets.**

***Index Terms*—Body-worn cameras, video quality, real-time processing.**

I. Introduction

Body-worn cameras are increasingly popular [1], [2], and their market is expected to reach USD 10.9 billion by 2025 [3]. Videos taken with body-worn cameras are often captured under uncontrolled conditions, without viewfinder and subject to abrupt motion of the wearer [4], which generate distortions such as overexposure, defocus and blur. Therefore, it is important to automatically estimate video quality prior to further processing, for example for object and action recognition, automatic tagging, search and editing. A challenge in automatically assessing the quality of videos from body-worn cameras is that distortions may considerably vary over time, thus making methods that assign a single score after processing the video [5] not applicable. Algorithms that operate on each frame or on short temporal windows are instead preferable [6].

A video quality assessment method can be full reference, reduced reference, mutual reference or no reference. Full and reduced reference methods assume that a distortion-free video is available to help identifying and quantifying the distortions. Full reference methods use the whole distortion-free frames [7], [8], while reduced reference methods use only partial information [9], such as features from a divisive normalisation transformation [10] or local entropy [11]. Mutual reference methods measure quality relative to *pseudo-reference* frames that contain overlapping content with the tested image, although not necessarily pixel-aligned [12]. Finally, no-reference methods use general properties of a *good* video [13] or measure typical distortions, such as blur, blocking artifacts or lack of *naturalness* [14]–[17].

No-reference methods can be classified as distortion-specific and non-distortion-specific [18]. Distortion-specific methods assume the type of distortion(s) to be known. For example, Just Noticeable Blur [19] quantifies sharpness in images with uniform saliency content and Cumulative Probability of Blur Detection [16] deals with non-uniform saliency content with a probabilistic model of blur perception with strong edges. Non-distortion-specific methods estimate frame quality using statistics on image indexing (e.g. Blind Image Quality Index [15]) and natural scenes (e.g. Distortion Identification-based Image Verity and INtegrity Evaluation [20]), or with probabilistic models of visual quality perception [21], [22]. Codebook Representation for No-Reference Image Assessment (CORNIA) [23] uses image patches as feature and soft-assignment coding with max pooling to characterise image distortions. Blind/Referenceless Image Spatial QUality Evaluator (BRISQUE) builds on the work of Ruderman [24] and describes image distortions with a set of coefficients integrated in a statistics-based model [14].

Unlike methods that employ Gabor filters, Wavelets or discrete cosine transform [10], [21], [25], [26], CORNIA and BRISQUE work directly in the spatial domain. BRISQUE is one order of magnitude faster than CORNIA [18]. However, the performance of BRISQUE is unsatisfactory with contrast distortions [27].

In this paper, we present M-BRISQUE, a no-reference non-distortion-specific video quality assessment method that works in real-time. We adopt the Michelson contrast [28] to account for distortions that are specific to body-worn camera videos and combine it with BRISQUE [14]. We designed the implementation as a set of concurrent parallel processes and compute M-BRISQUE on short temporal windows for on-line assessment. Our CPU implementation uses two multi-thread processes in

cascade and reaches real-time performance for videos at resolution 1920×1080 pixels, processed at 24 *Hz*. We show the application of M-BRISQUE for multi-view camera selection, and validate the predictor with a subjective evaluation on body-worn camera videos and on two public datasets.

The paper is organised as follows. Sec. II introduces M-BRISQUE, its application to multi-view content editing and its real-time implementation. Sec. III presents the experimental validation and Sec. IV draws the conclusions.

II. M-BRISQUE

A. The feature vector

Let $I(i,j)$ be the intensity of pixel (i,j), and I_{max} and I_{min} be the maximum and minimum intensity values in a frame. The Michelson contrast, C_m, is a frame-level score defined as [28]:

$$C_m = \frac{I_{max} - I_{min}}{I_{max} + I_{min}}. \tag{1}$$

The Mean Subtracted Contrast Normalised (MSCN) coefficients, $\hat{I}(i,j)$, describe locally the normalised luminance and vary coherently in the presence of a distortion, and are defined as [14], [24]:

$$\hat{I}(i,j) = \frac{I(i,j) - \mu(i,j)}{\sigma(i,j) + 1}, \tag{2}$$

with

$$\mu(i,j) = \sum_{k=-K}^{K} \sum_{l=-L}^{L} \omega_{k,l} I(i+k, j+l) \tag{3}$$

and

$$\sigma(i,j) = \sqrt{\sum_{k=-K}^{K} \sum_{l=-L}^{L} \omega_{k,l} \left(I(i+k, j+l) - \mu(i,j)\right)^2}, \tag{4}$$

where $\omega = \{\omega_{k,l} : k \in [-K, K], l \in [-L, L]\}$ is a circular-symmetric 2D Gaussian normalised to a unit value and sampled at 3 standard deviations.

The specific distortion can be estimated by fitting Generalised Gaussian Distribution (GGD) and Asymmetric Generalised Gaussian Distribution (AGGD) models to the histogram of the MSCN coefficients, based on the assumption that MSCN coefficients statistically present a Gaussian distribution in undistorted images [14], [24]. GGD is defined by shape, α, and variance, σ_g:

$$f(x; \alpha, \sigma_g^2) = \frac{\alpha}{2\beta\Gamma(\frac{1}{\alpha})} exp\left(-\left(\frac{|x|}{\beta}\right)^{\alpha}\right), \tag{5}$$

where $x = \hat{I}(i,j)$, $\beta = \sigma_g \sqrt{\Gamma(1/\alpha)/\Gamma(3/\alpha)}$ and $\Gamma(a) = \int_0^\infty t^{a-1} e^{-t} dt$ with $a > 0$. The distribution is zero mean and (α, σ_g^2) are estimated using moment-matching [14].

The zero-mode AGGD is obtained as

$$f(x; \nu, \sigma_l^2, \sigma_r^2) = \begin{cases} \frac{\nu}{(\beta_l + \beta_r)\Gamma(\frac{1}{\nu})} exp\left(-\left(\frac{-x}{\beta_l}\right)^{\nu}\right) & x < 0 \\ \frac{\nu}{(\beta_l + \beta_r)\Gamma(\frac{1}{\nu})} exp\left(-\left(\frac{x}{\beta_r}\right)^{\nu}\right) & x \geq 0 \end{cases} \tag{6}$$

with the left, β_l, and the right, β_r, scale parameters defined, respectively, as

$$\beta_l = \sigma_l \sqrt{\frac{\Gamma\left(\frac{1}{\nu}\right)}{\Gamma\left(\frac{3}{\nu}\right)}} \tag{7}$$

and

$$\beta_r = \sigma_r \sqrt{\frac{\Gamma(\frac{1}{\nu})}{\Gamma\left(\frac{3}{\nu}\right)}}, \tag{8}$$

where ν defines the shape of AGGC; and σ_l^2 and σ_r^2 define the horizontal and vertical variances, respectively. If $\sigma_l^2 = \sigma_r^2$ then AGGD reduces to GGD. The values of ν, σ_l^2, and σ_r^2 are estimated by moment-matching, as for GGD.

The four parameters characterising AGGD are η, ν, σ_l^2 and σ_r^2. The mean of AGGD is defined as

$$\eta = (\beta_r - \beta_l) \frac{\Gamma\left(\frac{2}{\nu}\right)}{\Gamma\left(\frac{1}{\nu}\right)}. \tag{9}$$

AGGD is calculated on four orientations of the MSCN coefficients:

$$\begin{aligned} H(i,j) &= \hat{I}(i,j)\hat{I}(i,j+1), \\ V(i,j) &= \hat{I}(i,j)\hat{I}(i+1,j), \\ D_1(i,j) &= \hat{I}(i,j)\hat{I}(i+1,j+1), \\ D_2(i,j) &= \hat{I}(i,j)\hat{I}(i+1,j-1), \end{aligned} \tag{10}$$

corresponding to horizontal, vertical and two diagonals orientations, respectively.

The resulting 37-dimensional M-BRISQUE feature vector is composed of C_m, and the two parameters for GGD, namely α and σ_g^2, and the 16 parameters for AGGD, namely η, ν, σ_l^2 and σ_r^2 calculated in four orientations, on two scales.

B. Mapping the feature values to human judgement

The M-BRISQUE score, s_k, at frame k is generated through a Support Vector Regression (SVR) trained with Radial Basis Function (RBF) kernels[1] [29], [30]. This provides the mapping between the feature vector presented in the previous section and human judgement, which we compute with the Spearman's Rank Ordered Correlation Coefficient (SROCC) [14] as objective function that operates in $[0, 1]$. To prevent overfitting, we perform cross validation.

We train M-BRISQUE on the Computational and Subjective Image Quality database [31], which consists of 30 original images and six distortions: JPEG and JPEG2000 compression, global *contrast* decrements, additive pink Gaussian noise, and Gaussian blurring. Figure 1 shows M-BRISQUE scores for a set of sample frames.

[1]SVR is implemented by LIBSVM https://www.csie.ntu.edu.tw/~cjlin/libsvm/, last accessed June 2018.

(a) 0.262 (b) 0.444 (c) 0.748

Fig. 1: M-BRISQUE score for sample frames from a body-worn camera video [4] (the lower M-BRISQUE, the better the quality): (a) good-quality frame, (b) overexposed and blurred, (c) heavily blurred.

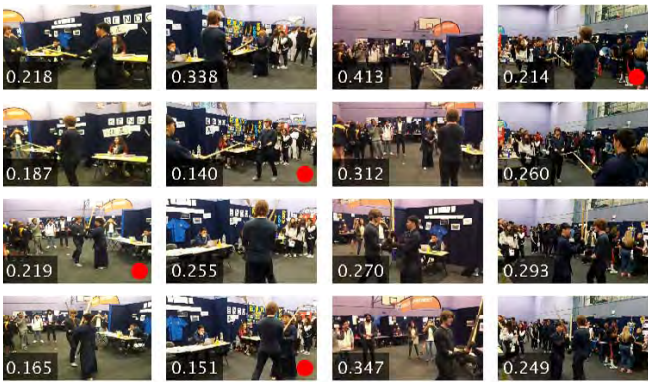

Fig. 2: Multi-view camera selection based on M-BRISQUE. Columns: different camera views; rows: scene captured from different views at the same time instant. The number overlaid on each frame is its M-BRISQUE score (the lower M-BRISQUE, the better the quality). The red dot indicates the selected view.

C. Application to view selection

M-BRISQUE can support, for example, multi-view camera selection applications. In such applications, videos of the same event recorded simultaneously are analysed to generate automatically a single video by selecting the best-quality view over time [32]. For simplicity, we switch among views every $T = 5$ seconds by selecting the best available view (excluding the currently selected view) defined by the mean M-BRISQUE score over the previous 0.5 seconds. Figure 2 shows sample frames from this application, indicating the selected view in four switching instances. Additional examples can be seen at [33].

D. Speed

M-BRISQUE is implemented as two multi-thread processes in cascade. The first thread deals with multiple input videos and considers each video as an independent source that concurrently accesses the available resources. The second thread deals with video quality assessment by three parallel processes that extract the 37-dimensional feature vector for each frame (see Fig. 3). Process 1 is for the Michelson Contrast, and the other two processes are for GGD and AGGD on the original image-size (process 2) and the halved image-size (process 3).

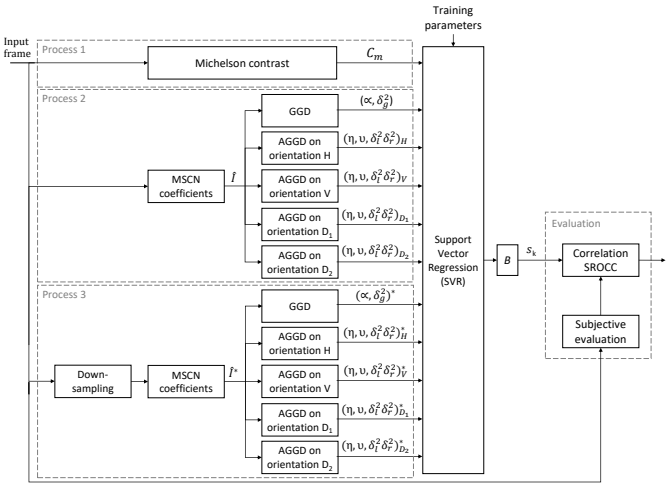

Fig. 3: Block diagram of the parallel processes for feature extraction in M-BRISQUE (the symbol "$*$" indicates variables obtained on the down-sampled image).

TABLE I: Speed of M-BRISQUE (Hz) when processing on a single CPU up to four videos playing simultaneously.

video resolution	number of videos			
	1	**2**	**3**	**4**
720×576	78.23	29.00	15.19	9.87
1280×720	42.75	16.39	8.13	5.00
1920×1080	24.39	8.13	4.27	2.54

M-BRISQUE performs video quality assessment in real time on a 3.4 GHz Intel Core i7 machine with 32 GB of memory. Table I shows the computational speed of M-BRISQUE when assessing on the same machine multiple videos at different resolutions.

A dynamic sampling controls how many frames per second the M-BRISQUE software can handle over time. We set the minimum sampling rate to 3 Hz and, in order to avoid fluctuations due to abrupt temporal variations, a buffer, B, of 15 frames stores the scores of each processed frame and the mean of these scores is considered. See [33] for a video with the screen-capture of a demo.

III. Validation

A. Experimental setup

We perform the experimental validation with a subjective test and three quality measures on two publicly available datasets, LIVE Image Quality Assessment Database (IQAD) [34] and LIVE Mobile In-Capture Video Quality Database (MICVQD) [35].

IQAD consists of 982 images with five distortion types. We only consider distortions that are relevant to our problem, namely white noise, Gaussian blur and simulated fast fading Rayleigh channel. This selection results in 522 test images.

MICVQD consists of 208 videos captured with eight hand-held mobile devices, and categorised into six distortions typically occurring with amateur recordings and

TABLE II: Spearman's Rank Ordered Correlation Coefficient between objective scores and subjective judgements on the LIVE Image Quality Assessment Database (IQAD) [34] and the LIVE Mobile In-Capture Video Quality Database (MICVQD) [35] for different distortions.

	IQAD			MICVQD					
Method	**White noise**	**Gaussian blur**	**Fast fading**	**Artifacts**	**Colour**	**Exposure**	**Focus**	**Sharpness**	**Stabilisation**
RMS	.191	.045	.011	.007	.171	.026	.147	.007	.134
Michelson Contrast	.510	.063	.094	.400	.130	.473	.080	**.580**	.280
BRISQUE	.900	**.752**	.628	**.601**	.328	.492	.301	.451	**.513**
M-BRISQUE	**.932**	.534	**.786**	.558	**.516**	**.601**	**.358**	.544	.508

(a) 0.345 (b) 0.107 (c) 0.466

(d) 0.047 (e) 0.426 (f) 0.461

(g) 0.685 (h) 0.452 (i) 0.225

(j) 0.268 (k) 0.350 (l) 0.180

Fig. 4: Sample frames and their corresponding M-BRISQUE scores (a-b) artifacts, (c-d) colour, (e-f) exposure, (g-h) focus, (i-j) sharpness, and (k-l) stabilisation (the labels of the distortions are defined in [35]).

in body-worn camera videos (given the presence of simultaneous distortions in the videos, the most evident is considered for the categorisation [35]). The distortions are (see Fig. 4): noise, blockiness and distortions not related to video content (*artifacts*); incorrect or insufficient colour representation (*colour*); over/under exposed regions (*exposure*); out-of-focus distortions (*focus*); general lack of details, texture or sharpness (*sharpness*); and for camera shake (*stabilisation*).

B. Comparison of quality measures

We compare M-BRISQUE with BRISQUE [14], Michelson Contrast and RMS [5], and we correlate through SROCC the score of each method with the subjective quality scores provided with the datasets (the ground truth for our experiments), similarly to [14], [22].

All methods are trained on the Computational and Subjective Image Quality database, as M-BRSQUE, using a cross validation with 80% training and 20% testing on 100 random runs. $K = L = 3$ [14] in our experiments.

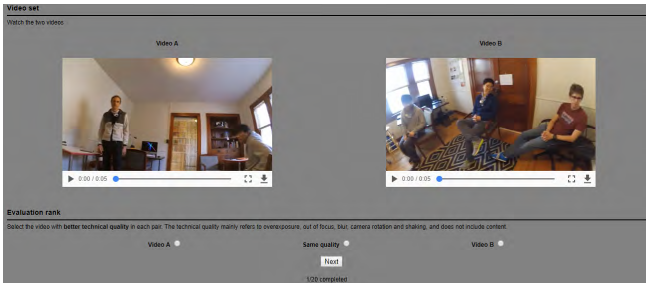

Fig. 5: The interface used for the subjective evaluation.

Table II shows the mean score of all images on IQAD and MICVQD, with MICVQD being generally a more challenging dataset compared to IQAD, as expected. BRISQUE outperforms the other methods in 2 out of 3 distortions in IQAD and 3 out of 6 distortions in MICVDQ. Interestingly, the Michelson Contrast alone performs well in more than half of all distortions. These results show how, on average, the best performance is obtained by a combination of local (BRISQUE) and global (Michelson Contrast) cues.

C. Subjective experiment

We also validate M-BRISQUE with a double-stimulus subjective evaluation (Fig. 5), using a setup similar to [12]. Subjects were asked to *select the video with* ***better technical quality*** *in each pair. The technical quality mainly refers to overexposure, out of focus, blur, camera rotation and shaking, and does not include content.*

The dataset comprises 16 clips, of 5 seconds each, obtained from the body-worn camera videos of the set 7 of the *1st-3rd* dataset [4] (sample frames can be seen in Fig. 1). As quality may considerably vary over time, we choose clips whose M-BRISQUE score is contained within a 10% variation during the clip. We randomly select 18 clip pairs and also add two pairs as duplicate of a previous pair, but with videos displayed in inverted positions (left to right and vice versa) to check the consistency of judgement. There are therefore 20 video pairs to evaluate.

A total of 28 subjects participated in the experiment (18 males and 10 females). The choice *same quality* videos was also an option leading to 33% chance for each choice with a random classifier. The *same quality* option was selected four times per test on average. The experiment revealed the difficulty in judging the (technical) quality of body-worn camera videos as subjects inconsistently marked the

two duplicated pairs 39% of the time (of which 55% of the time included a *same quality* judgement and 45% of the time consisted in a swapping of the preferred video). The M-BRISQUE scores agree with the subjective choices 45% of the time, calculated on the 18 pairs.

IV. Conclusion

We presented M-BRISQUE, a real-time video quality assessment method based on the Michelson contrast and BRISQUE. M-BRISQUE achieves good performance on the LIVE Image Quality Assessment Database (IQAD) [34] and LIVE Mobile In-Capture Video Quality Database (MICVQD) [35]. As future work, we will use short-term temporal information across frames and expand the pool of videos for the subjective test.

References

[1] C. Bai and A. Reibman, "Characterizing distortions in first-person videos," in *Proc. of IEEE Int. Conf. on Image Processing*, Phoenix, USA, 25–28 Sep 2016, pp. 2440–2444.

[2] A. Lidon, M. Bolaños, M. Dimiccoli, P. Radeva, M. Garolera, and X. Giró-i Nieto, "Semantic summarization of egocentric photo stream events," in *Proc. of ACM Multimedia Workshop*, Mountain View, USA, 23–27 Oct 2017.

[3] "https://www.grandviewresearch.com/industry-analysis/wearable-camera-market," (last accessed Jun 2018).

[4] C. Fan, J. Lee, M. Xu, K. Singh, Y. Lee, D. Crandall, and M. Ryoo, "Identifying first-person camera wearers in third-person videos," in *Proc. of IEEE Conf. on Computer Vision and Pattern Recognition*, Honolulu, Hawaii, USA, 21–26 Jun 2017, pp. 4734–4742.

[5] P. Vu and D. Chandler, "ViS3: an algorithm for video quality assessment via analysis of spatial and spatiotemporal slices," *Journal of Electronic Imaging*, vol. 23, pp. 23–23–25, 2014.

[6] M. Torres Vega, D. Mocanu, and A. Liotta, "Unsupervised deep learning for real-time assessment of video streaming services," *Multimedia Tools and Applications*, vol. 76, no. 21, pp. 22 303–22 327, Nov 2017.

[7] X. Zhang, X. Feng, W. Wang, and W. Xue, "Edge strength similarity for image quality assessment," *IEEE Signal Processing Letters*, vol. 20, no. 4, pp. 319–322, Apr 2013.

[8] C. Charrier, O. Lézoray, and G. Lebrun, "Machine learning to design full-reference image quality assessment algorithm," *Signal Processing: Image Communication*, vol. 27, no. 3, pp. 209–219, 2012.

[9] L. Ma, S. Li, F. Zhang, and K. Ngan, "Reduced-reference image quality assessment using reorganized DCT-based image representation," *IEEE Trans. on Multimedia*, vol. 13, no. 4, pp. 824–829, Aug 2011.

[10] A. Rehman and Z. Wang, "Reduced-reference image quality assessment by structural similarity estimation," *IEEE Trans. on Image Processing*, vol. 21, no. 8, pp. 3378–3389, Aug 2012.

[11] C. Bampis, P. Gupta, R. Soundararajan, and A. Bovik, "SpEED-QA: Spatial efficient entropic differencing for image and video quality," *IEEE Signal Processing Letters*, vol. 24, no. 9, pp. 1333–1337, Sep 2017.

[12] C. Bai and A. Reibman, "Mutual reference frame-quality assessment for first-person videos," in *Proc. of IEEE Int. Conf. on Image Processing*, Beijing, China, 17–20 Sep 2017, pp. 290–294.

[13] H. Wu and K. Rao, *Digital Video Image Quality and Perceptual Coding (Signal Processing and Communications)*. Boca Raton, FL, USA: CRC Press, Inc., 2005.

[14] A. Mittal, A. Moorthy, and A. Bovik, "No-reference image quality assessment in the spatial domain," *IEEE Trans. on Image Processing*, vol. 21, no. 12, pp. 4695–4708, Dec 2012.

[15] A. Moorthy and A. Bovik, "A two-step framework for constructing blind image quality indices," *IEEE Signal Processing Letters*, vol. 17, no. 5, pp. 513–516, May 2010.

[16] N. Narvekar and L. Karam, "A no-reference image blur metric based on the cumulative probability of blur detection (CPBD)," *IEEE Trans. on Image Processing*, vol. 20, no. 9, pp. 2678–2683, Sep 2011.

[17] Y. Zhang and D. Chandler, "An algorithm for no-reference image quality assessment based on log-derivative statistics of natural scenes," *Proc. of SPIE*, vol. 8653, pp. 8653–10, 2013.

[18] R. Manap and L. Shao, "Non-distortion-specific no-reference image quality assessment: A survey," *Information Sciences*, vol. 301, no. Supplement C, pp. 141–160, Apr 2015.

[19] R. Ferzli and L. Karam, "A no-reference objective image sharpness metric based on the notion of just noticeable blur (JNB)," *IEEE Trans. on Image Processing*, vol. 18, no. 4, pp. 717–728, Apr 2009.

[20] A. Moorthy and A. Bovik, "Blind image quality assessment: From natural scene statistics to perceptual quality," *IEEE Trans. on Image Processing*, vol. 20, no. 12, pp. 3350–3364, Dec 2011.

[21] M. Saad, A. Bovik, and C. Charrier, "Blind image quality assessment: A natural scene statistics approach in the DCT domain," *IEEE Trans. on Image Processing*, vol. 21, no. 8, pp. 3339–3352, Aug 2012.

[22] K. Gu, G. Zhai, X. Yang, and W. Zhang, "Using free energy principle for blind image quality assessment," *IEEE Trans. on Multimedia*, vol. 17, no. 1, pp. 50–63, Jan 2015.

[23] P. Ye, J. Kumar, L. Kang, and D. Doermann, "Unsupervised feature learning framework for no-reference image quality assessment," in *Proc. of IEEE Conf. on Computer Vision and Pattern Recognition*, Providence, Rhode Island, USA, 16–21 Jun 2012, pp. 1098–1105.

[24] D. Ruderman, "The statistics of natural images," *Network: Computation in Neural Systems*, vol. 5, no. 4, pp. 517–548, 1994.

[25] R. Hong, J. Pan, S. Hao, M. Wang, F. Xue, and X. Wu, "Image quality assessment based on matching pursuit," *Information Sciences*, vol. 273, no. Supplement C, pp. 196–211, 2014.

[26] X. Li, Q. Guo, and X. Lu, "Spatiotemporal statistics for video quality assessment," *IEEE Trans. on Image Processing*, vol. 25, no. 7, pp. 3329–3342, Jul 2016.

[27] K. Gu, W. Lin, G. Zhai, X. Yang, W. Zhang, and C. Chen, "No-reference quality metric of contrast-distorted images based on information maximization," *IEEE Trans. on Cybernetics*, vol. 47, no. 12, pp. 4559–4565, Dec 2017.

[28] H. Kukkonen, J. Rovamo, K. Tiippana, and R. Nasanen, "Michelson contrast, RMS contrast and energy of various spatial stimuli at threshold," *Vision Research*, vol. 33, no. 10, pp. 1431–1436, 1993.

[29] B. Schölkopf, A. Smola, R. Williamson, and P. Bartlett, "New support vector algorithms," *Neural Computation*, vol. 12, no. 5, pp. 1207–1245, May 2000.

[30] M. Narwaria and W. Lin, "Objective image quality assessment based on support vector regression," *IEEE Trans. on Neural Networks*, vol. 21, no. 3, pp. 515–519, Mar 2010.

[31] E. Larson and D. Chandler, "Most apparent distortion: full-reference image quality assessment and the role of strategy," *Journal of Electronic Imaging*, vol. 19, pp. 19–21, 2010.

[32] S. Bano and A. Cavallaro, "ViComp: composition of user-generated videos," *Multimedia Tools and Applications*, vol. 75, no. 12, pp. 7187–7210, Jun 2016.

[33] "http://cis.eecs.qmul.ac.uk/projects/MBRISQUE," (last accessed Jun 2018).

[34] H. Sheikh, M. Sabir, and A. Bovik, "A statistical evaluation of recent full reference image quality assessment algorithms," *IEEE Trans. on Image Processing*, vol. 15, no. 11, pp. 3440–3451, Nov 2006.

[35] D. Ghadiyaram, J. Pan, A. Bovik, A. Moorthy, P. Panda, and K. Yang, "Subjective and objective quality assessment of mobile videos with in-capture distortions," in *Proc. of IEEE Int. Conf. on Acoustics, Speech and Signal Processing*, New Orleans, USA, 5–9 Mar 2017, pp. 1393–1397.